Synthesis and SARs of dopamine derivatives as potential inhibitors of influenza virus PA_N endonuclease

Yixian Liao, Yilu Ye, Sumei Li, Yilian Zhuang, Liye Chen, Jianxin Chen, Zining Cui, Lijian Huo, Shuwen Liu, Gaopeng Song

PII: S0223-5234(20)30015-5

DOI: https://doi.org/10.1016/j.ejmech.2020.112048

Reference: EJMECH 112048

To appear in: *European Journal of Medicinal Chemistry*

Received Date: 25 November 2019

Revised Date: 7 January 2020

Accepted Date: 7 January 2020

Please cite this article as: Y. Liao, Y. Ye, S. Li, Y. Zhuang, L. Chen, J. Chen, Z. Cui, L. Huo, S. Liu, G. Song, Synthesis and SARs of dopamine derivatives as potential inhibitors of influenza virus PA_N endonuclease, *European Journal of Medicinal Chemistry* (2020), doi: https://doi.org/10.1016/j.ejmech.2020.112048.

Synthesis and SARs of dopamine Derivatives as Potential Inhibitors of Influenza Virus PA_N Endonuclease

Yixian Liao[a, b*,1], Yilu Ye[c ,1], Sumei Li[d], Yilian Zhuang[a], Liye Chen[a], Jianxin Chen[e], Zining Cui[b], Lijian Huo[a], Shuwen Liu[c*], Gaopeng Song[a*]

[a]*College of Materials and Energy, South China Agricultural University, Guangzhou, 510642, China*

[b]*State Key Laboratory for Conservation and Utilization of Subtropical Agro-bioresources, Integrative Microbiology Research Centre, Guangdong Province Key Laboratory of Microbial Signals and Disease Control, South China Agricultural University, Guangzhou 510642, China*

[c]*School of Pharmaceutical Sciences, Southern Medical University, Guangzhou, 510515, China*

[d]*Department of human anatomy, School of Medicine, Jinan University, Guangzhou, 510632, China*

[e]*Guangdong Provincial Key Laboratory of Veterinary Pharmaceutics Development and Safety Evaluation, College of Veterinary Medicine, South China Agricultural University, Guangzhou 510642, China*

Abstract: Currently, influenza PA_N endonuclease has become an attractive target for development of new drugs to treat influenza infections. Herein we report the discovery of new PA_N endonuclease inhibitors derived from a chelating agent dopamine moiety. A series of dopamine amide derivatives and their conformationally constrained 1,2,3,4-tetrahydroisoquinoline-6,7-diol-based analogs were elaborated and assayed against influenza virus A/WSN/33 (H1N1). Most compounds exhibited moderate to excellent antiviral activities, generating a preliminary SARs. Among them, compounds **14** and **19** showed stronger anti-IAV activity compared with the reference Peramivir. Moreover, **14** and **19** demonstrated a concentration-dependent inhibition of PA_N endonuclease based on both FRET assay and SPR assay. Docking studies were also performed to elucidate the binding mode of **14** and **19** with the PA_N protein and to identify amino acids involved in their mechanism of action, which were well consistent with the biological data. This finding was beneficial to laying the foundation for the rational development of more effective PA_N endonuclease inhibitors.

Keywords: Influenza A virus; PA_N endonuclease inhibitors; polyphenols; SARs

1. Introduction

Influenza A viruses (IAVs) are associated with occasional pandemics that usually

* Corresponding author. Tel.: +86- 20- 6164 8538; fax: +86 -20 -6164 8655
E-mail address: liusw@smu.edu.cn (S. Liu).
* Corresponding author. Tel.: + 86-20-85280293; fax: + 86-20-85280292
E-mail address: songgp1021@scau.edu.cn (G. Song).
[1]These authors contributed equally to this work

cause contagious pandemic respiratory illnesses, high morbidity and mortality rates [1-2]. Currently, two classes of antiviral drugs have been clinically used that comprise the M2 protein blockers (amantadine and rimantadine) and neuraminidase (NA) inhibitors (oseltamivir and zanamivir). However, the growing resistance to above approved drugs underlines the need for the development of novel therapeutics with different mechanisms of action on viral life cycles [3-5].

IAVs belong to the *Orthomyxoviridae* family, and its genome consists of segmented single stranded RNA (-) that encodes ten different viral protein [6,7]. Thereinto, the three largest RNA segments encode three subunits of viral RdRP: polymerase acidic protein (PA), polymerase basic protein 1 (PB1) and polymerase basic protein 2 (PB2) [8]. At the beginning of replication, the PB2 subunit binds the 5'-mRNA cap of a host cell, and in the second step the PA subunit cleaves 10-13 nucleotides downstream to yield 5'-capped RNA fragments. These fragments serve as primers for viral mRNA elongation catalyzed by the PB1 subunit in the third step [9].

PA_N endonuclease is highly conserved across all influenza strains and subtypes and has no human analogue [10]. Currently, PA_N protein has represented an attractive target for new antiviral drugs. Studies have demonstrated that PA_N domain contains the endonuclease active site where a dinuclear metal active site, employing two Mn^{2+} or Mg^{2+} cations, is critical for the endonuclease activity [11]. Thus, PA_N endonuclease inhibitors that coordinate the metal centers of the endonuclease active site, can effectively inhibit endonuclease activity and prevent the processing of the biological substrates. To date, several series of direct PA_N endonuclease inhibitors have been reported in recent literature that can be chemically classified as diketo acid derivatives [12-15], catechol derivatives [16], flutimide derivatives [17,18], hydroxylated heterocycles (3-hydroxyquinolin-2(1H)-ones, and other scaffolds) [19-23]. Notably,

Xofluza, a typical hydroxylated heterocycles, has been used in clinic in Japan and approved by FDA in October 2018, which is a highly selective and nontoxic inhibitor without interfering with function of the host cell [24, 25]. However, widely use of Xofluza will prompt the influenza A virus PA-I38T variants such as H3N2 and A/H1N1pdm [26], which confers reduced susceptibility to Xofluza without a loss of viral fitness. Moreover, the variants also transmitted efficiently between ferrets by respiratory droplets [26]. Considering this, there is an urgent need for the development of novel PA_N endonuclease inhibitors to prevent and treat the influenza infection.

Of particular interest, polyphenols have gained a lot of attention due to their broad efficacy against influenza PA_N endonuclease [27, 28]. For example, polyphenols such as tea catechin (**1**), marchantin B (**2**), perrottetin F (**3**), phenethylphenylphthalimide analog (**4**), salicylic acid derivative (**5**) and gallic acid derivative (**6**) (Figure 1) have been found to modulate PA endonuclease function [27-30]. Structurally, all of the above polyphenols possess a catechol moiety, indicating its crucial role in the PA_N endonuclease inhibitory activity. This finding was further confirmed based on the co-crystal of the PA_N endonuclease with (-)-epigallocatechin gallate (**1**) [13], in which the two manganese ions were cochelated with two of the hydroxyl groups of the gallo group in deep active site cleft. However, most of polyphenols derivatives produced only modest or weak anti-IAV activity (EC_{50} > 15 μM) in the host cells, despite their reasonable PA_N endonuclease inhibition activity.

Insert < Figure 1>

Given the SARs of above polyphenols derivatives, we recognized that there are

several key pharmacophoric regions where appropriate substituents are essential (Figure 2). a) 3,4-dihydroxyphenethyl moiety is indispensable, whereas an additional aromatic moiety is important at the *para*-position of 3,4-dihydroxyphenethyl fragment through appropriate linkers. b) In general, the length of linkers was less than 4 C. c) both different substituents such as fluorine, chlorine and the aromatic moiety could bind to the active pocket via hydrophobic interaction. Encouragingly, the dihydroxyindole derivative **7** as an effective PA_N endonuclease inhibitor displayed remarkable anti-IAV activity in MDCK cells (EC_{90} = 3.2 μM), of which both hydroxyl groups on the dihydroxyindole moiety chelated two metal ions and the catechol functional group was engaged in the Val122-Arg124-Tyr130 cavity that is of crucial importance [31]. Careful analysis of docking studies on the endonuclease with **7** and its analogues, we inferred that not only the active site of PA protein can accommodate aromatic molecules connected by longer linkage (more than 3 C), but also there is a preference for the aromatic molecules with hydroxyl groups, which may also make very favorable interactions with amino acids in hydrophobic pockets.

Insert < Figure 2>

More recently, Ferro et al carried out a three-dimensional pharmacophore model and found the dopamine moiety (3,4-dihydroxyphenethylamine) seemed a great fragment capable of chelating the two metal ions [32]. Guided by both the above SARs outlined in Figure **2** and prior docking studies, we started our structure modification study of dopamine moiety to design the title series A (**8**-**17**). Initial efforts focused on exploring aryl amides **8-13** derived from the coupling of dopamine and several hydroxybenzoic acids. With the aim to investigate the influence of

linkage-length on antiviral activity, introduction of methylene or ethylene spacers between the amide and aryl ring gave rise to derivative **14** or **15**, respectively. Moreover, compounds **16** and **17**, bioisosteric surrogates of **14**, were designed to study the effects of type of linkages on antiviral activity. Considering the conformational restriction has been frequently introduced to some structurally flexible ligands for optimizing the biological activity and specificity [33, 34], we prepared the title series B (**18-20**) by replacing the flexible dopamine with 1,2,3,4-tetrahydroisoquinoline-6,7-diol fragment that bears more conformational rigidity. Herein, we report an extensive SARs study leading to the identification of the lead compound **14** with potential antiviral activity *in vitro* (EC_{50} = 2.5 μM for WSN33) and excellent PA_N endonuclease inhibition (IC_{50} = 0.3 μM).

Insert < Figure 3>

2. Results and discussion

2.1. Chemistry

Synthesis of dopamine derivative derivatives **8-15** and 1,2,3,4-tetrahydroisoquinoline-6,7-diol **18-20** from commercially available 3,4-dihydroxybenzaldehyde was outlined in Scheme 1. The phenolic hydroxyl groups of **21** were selectively protected as a benzyl ether by treatment with benzyl bromide in the presence of potassium carbonate to yield **22**. The intermediate **23** was derived from **22** and then reduced to benzyl-protected dopamine **24** using lithium aluminum hydride. Condensation of various carboxylic acid followed by selective hydrogenolysis of benzyl ether over palladium/carbon furnished **8-15** in good yields. 1,2,3,4-Tetrahydroisoquinoline ring **33** was accomplished via the Pictet-Spengler

reactions. Amide derivatives **18-20** were generated by the coupling of various acids to **33**, followed by hydrogenolysis of benzyl ether.

Insert <Scheme 1>

Derivative **16** was done by the similar route as that for compound **14** from the known compound **37**, as shown in Scheme 2. Consider palladium carbon was sensitive to sulfur element, the commercially available 2-(3,4-dimethoxyphenyl)ethan-1-amine **38** was treated with the known 2-(3,4-dimethoxyphenyl)acetic acid in the presence of EDC•HCl and DMAP to give **40**, which was subject to Lawesson's reagent to provide thioamide intermediate **41**. Hydrolysis of methoxy groups in the presence of BBr_3 efficiently afforded **17**.

Insert <Scheme 2>

2.2. Biological assays

*2.2.1. Anti-influenza virus activity of polyphenol derivatives **8-20***

The cytopathic effect (CPE) assay and the antiviral effect quantitatively evaluated with the cell-based MTT assay were utilized in parallel to demonstrate their antiviral abilitiws of these polyphenols derivatives **8-20** [35]. And the cytotoxicity of polyphenols derivatives was assessed by the 3-[4,5-dimethylthiazol-2-yl]-2,5-diphenyl tetrazolium bromide (MTT) assay [36]. As shown in Figure 4, compound **14** dramatically reduced the CPE in 20 μM, indicating that these polyphenols derivatives were able to protect MDCK cells from influenza virus-induced CPE. Among them, **14** displayed the strongest antiviral activity (see

Table 1) and had an increased 2-fold or 12-fold cellular activity than the control Peramivir or EGCG, respectively.

Insert <Figure 4>

Firstly, we analysed the effect of binding hydroxyl group in different positions of the second phenyl ring, *ortho*- (**8**, EC_{50} > 20.0 μM), *meta*- (**9**, EC_{50} = 13.1 μM) and *para*- (**10**, EC_{50} = 12.7 μM), suggesting the importance of this structural modification for antiviral activity. Specifically, moving the *para*-OH substituent to the *meta*- or *ortho* -position on the second phenyl ring resulted in a slightly decreased or total loss of activity, revealing that the hydroxyl substitution at the *para*-position of the phenyl ring was indispensable and the most optimal substituent for this position. There was a similar trend in 2,3-dihydroxyl substitution (**11**) as that of *ortho*-OH analogue **8**, probably due to the presence of intramolecular hydrogen bond formed by *ortho*-OH and carbonyl group. Of particular interest, 3,4-dihydroxyl substitution compound (**12**) showed enhanced inhibition over monosubstituted **9** or **10**. With the identification of potent analog **12** with 3,4-dihydroxyl substitution, we attempted to attach a third hydroxyl group in the *meta*-position of the second phenyl ring. However, 3,4,5-trihydroxyl derivative **13** exhibited a significant loss of activity relative to the disubstituted compound **12**. As observed, both the position and number of the substituents in the second phenyl ring were responsible for the potentiation of antiviral activity. Having optimized the different positions of the phenyl ring, we turned our attention to both the length and type of linkers. Comparing the anti-IAV activity of **14** or **15** with **12**, it was found that the length of the carbon chain (n) from 0 to 2 resulted in a substantial increase in potency though there was no correlation

between the length of the carbon chain and antiviral activity. The activity in the order of compounds **14** > **15** > **12** revealed that 3,4-dihydroxyphenylmethylene (n =1) was the most potent elaboration at this position, likely owing to both favorable hydrophobic interactions with pocket 3 or 4 (Fig. **7**) and possible additional hydrogen bond interactions with key hydrophilic residues on the external surface. Most importantly, **14** not only exhibited the best anti-IAV activity among this set of compounds, but also the remarkablly improved selective index (CC_{50}/EC_{50}) comparable to **12**. We next explored the linkage moiety by replacement of amide with ester or thioamide and found such a small change substantially had an important effect on anti-IAV activity (**14** vs **16**, **14** vs **17**). The CPE assay demonstrated that **17**, an analogue of **14**, in which an amide bond was replaced by the ester link had a slightly reduced potency compared to **14**, indicating the compatibility of amide and ester linkers for anti-A/WSN/33 virus. However, replacement of the amide group in **14** by the thioamide group, yielding **16**, led to the total loss of activity, revealing that the crucial nature of the amide linkage for anti-IAV activity. This result indicated that both the style and length of the linkers were a critical factor for antiviral activity.

Insert <Table 1>

With **12**, **14**, **15** as our most potent analogs in the series A, we made other push to enhance inhibition by restricting conformational freedom with a planarizing fusion of the catechol fragment and primary amine to furnish the 1,2,3,4-tetrahydroisoquinoline derivatives **18**-**20**. Surprisingly, compound **18** displayed a significant 3-fold increase in potency compared with the open-chain congener **12**. Of the other two analogues **19**-**20**, **19** performed slightly less

comparable with **14**, whereas **20** showed approximately 4-fold decreased activity than **15**. However, restricting conformational modification was detrimental for selective index (Table 2). Base on this result, we envisioned that restriction of rotation across the amide linkage might be crucial for antiviral activity and 1,2,3,4-tetrahydroisoquinoline derivatives maybe bind different regions and key amino acids in PA endonuclease active site from open-chain analogues in the series A.

Insert <Table 2>

2.2.2. The title compounds targeted PA_N endonuclease

In the next stage, compounds **14-15** and **17-19** were subjected to PA_N endonuclease enzymatic assay using fluorescence resonance energy transfer (FRET) inhibition assay [37, 38]. As shown in Table 3, the most potent antiviral compounds **14** and **19** within this series, exhibited stronger inhibition against the endonuclease activity than other three analogs, yielding EC_{50} values of 312.36 nM and 489.39 nM, respectively, which were superior to EGCG (EC_{50} = 6454.75 nM) but inferior to Baloxavir acid (BXA) (EC_{50} = 1.37 nM). As depicted in Figure 5A and 5B, a concentration-dependent inhibitory effect of compound **14** or **19** was observed on the PA_N endonuclease, which was similar to that of the positive control EGCG (Figure S1A) or BXA (Figure S1B). The good correlation between the results from the enzymatic assay and cell-based methods supported our hypothesis that the anti-IAV activity of compound **14** or **19** in cell culture was related to inhibition of PA-Nter.

Insert <Table 3>

Insert <Figure 5>

Considering that PA_N protein is a valuable target to develop antiviral agents, the possible interaction between **14** or **19** and influenza PA_N protein was further evaluated using SPR spectroscopy. It was found that compounds **14** and **19** immobilized on the Photo-cross-linker Sensor CHIP could bind tightly to PA_N endonuclease at concentrations of 10-160 nM, which was observed in a dose-dependent manner. As shown in Figure 6, **14** and **19** exhibited potential binding affinity to PA_N protein with K_D values of 26.33 nM and 94.19 nM, respectively, which was substantially higher relative to EGCG (Figure S2A, K_D = 956.32 nM) but lower than BXA (K_D = 207.51 pM, Figure S2B). In the light of these findings, it was reasonable to assume that **14** and **19** had the ability to exert anti-influenza activity by targeting PA_N endonuclease.

Insert <Figure 6>

2.2.3. Molecular docking analysis

In view of PA_N endonuclease as the potential target, we designed molecular docking calculations of compounds **14** and **19** with influenza PA_N endonuclease to further understand the molecular basis of the inhibitory properties of polyphenols derivatives through Surflex-Dock program in SYBYL 7.3 [39]. The optimum docked conformations of PA-compounds were determined based on the Total_Score and CSCORE. Hence, the selected compound **14** or **19** was docked into the published structure of H1N1 PA_N endonuclease bound with BXA (PDB: 6FS6) [40].

Our result indicated that either the dopamine moiety or 1,2,3,4-tetrahydroisoquinoline-6,7-diol fragment was able to direct toward to PA_N endonuclease active site for metal chelation and form hydrophobic contact with the

key residue His41. Specifically, it was found that the hydroxyl in 4-position of dopamine moiety could not only chelate with two catalytic metal ions but also form a hydrogen bond with the key residues Asp108 while the 3-hydroxyl substituent of dopamine could chelate with Mn1. As we have hypothesized above, the 3,4-dihydroxyphenylacetamide moiety of **14** was able to fit well into pocket 3, with the aryl ring making hydrophobic interactions with Tyr24 and the hydroxyl in *para*-position making a favorable hydrogen bond to Glu26. In contrast, the 1,2,3,4-tetrahydroisoquinoline-6,7-diol fragment was found to be too rigid to allow for chelating simultaneously with two catalytic metal ions but allow for orientating toward the pocket 4 and forming double hydrogen bonds with Ser194. Moreover, the aryl ring in **19** was able to form multiple hydrophobic contacts with Lys34 and Ala134, indicating that the larger size and greater number of available hydrophobic contacts and hydrogen interactions may account for the retained similar inhibitory activity as **14**, although with slightly less intensity of metal-ligand interactions than **14**. Of note, neither **14** nor **19** could form contact with Ile38. Therefore, we hypothesized that **14** or **19** might not change their binding affinity with PA_N endonuclease with I38T mutation.

Insert <Figure 7>

3. Conclusions

With the aim of developing a new class of PA_N endonuclease inhibitors, we designed and synthesized liner dopamine amide derivatives and 1,2,3,4-tetrahydroisoquinoline-6,7-diol-based conformationally constrained analogs, respectively, of which anti-IAV activities were evaluated in MDCK cells. The bioactivity results allowed for the generation of a preliminary SARs. The presence of

catechol moiety chelated to manganese ions was crucial for activity retention and both the position and number of the hydroxyl substituents in the second phenyl ring were responsible for the potentiation of anti-IAV activity, with the simultaneous replacement in the position *meta*- and *para*-positions most favorable. Both the style and length of the amide linkages played a key influence on antiviral activity. Conversion of the dopamine to 1,2,3,4-tetrahydroisoquinoline-6,7-diol ring led to an increase in cytotoxicity while keeping antiviral potency. Among all compounds tested, **14** and **19** exhibited comparable anti-IAV activity in relative to the reference Peramivir with a high SI. Based on FRET assay and SPR assay, the most potential **14** and **19** were found to show good antiviral ability by binding PA_N endonuclease, consistent well with the analysis result of docking study. To summarize, **14** and its active derivatives are promising antiviral agents that should be further investigated to develop new PA_N endonuclease inhibitors with preclinical relevance.

4. Experimental section

4.1. Chemistry: General Methods.

All reactions, unless otherwise stated, were done under nitrogen atmosphere. Reaction monitoring and follow-up were done using precoated E. Merck silica gel 60 F254 plates, visualizing with ultraviolet light. Flash column chromatography was done on silica gel (200-300 mesh, Qingdao, China) using petroleum ether, ethyl acetate, dichloromethane and methanol. The ^{1}H (600 MHz) and ^{13}C (150 MHz) NMR spectra were done in $CDCl_3$ and DMSO-d_6 and recorded on a JEOL JNM-ECP 600 spectrometer with tetramethylsilane as an internal standard, and chemical shifts were recorded in ppm values. Mass spectra were recorded on a Q-TOF Global mass spectrometer.

*4.2. 3,4-Bis(benzyloxy)benzaldehyde (**22**)*

To a solution of 3,4-dihydroxybenzaldehyde (5.0 g, 36.20 mmol), potassium carbonate (20.1 g, 144.80 mmol) in DMF (100 mL) was added benzyl bromide (17.19 mL, 144.80 mmol) at room temperature. The mixture was heated to 65 ºC for 10 h. After cooling, the solvent was evaporated under vacuum. The residue was partitioned between EtOAc and water. The combined organic layers were washed with brine, dried over Na_2SO_4, filtered and concentrated under reduced pressure. The crude product was purified by silica gel chromatography [EtOAc : petroleum ether : CH_2Cl_2, 15 : 1 : 1] to afford **22** as a white solid (11.10 g, 96%). ^{1}H NMR (600 MHz, Chloroform-*d*) δ 9.83 (s, 1H, Ar-CHO), 7.51 (d, 1H, *J* = 1.9 Hz, Ar-H), 7.50-7.45 (m, 4H, Ar-H), 7.43 (dd, 1H, *J* = 8.2, 1.9 Hz, Ar-H), 7.42-7.38 (m, 4H, Ar-H), 7.37-7.32 (m, 2H, Ar-H), 7.04 (d, 1H, *J* = 8.2 Hz, Ar-H), 5.28, 5.23 (each s, each 2H, Ar-CH_2-O); ESIMS: calcd for $[M+H]^+$ *m/z* 319.1; found, 319.1.

*4.3. (E)-(((4-(2-Nitrovinyl)-1,2-phenylene)bis(oxy))bis(methylene))dibenzene (**23**)*

A mixture of **22** (11.52 g, 36.18 mmol) and nitromethane (5.81 mL, 108.54 mmol) in glacial acetic acid (35 mL) was stirred at r. t. Then ammonium acetate (2.79 g, 36.18 mmol) was added and the mixture was stirred at 90 ºC for 5 h. After removing the solvents under vacuum, the residue was poured into water and extracted with EtOAc. The combined organic layers were washed with brine, dried over Na_2SO_4, filtered and evaporated. The crude product was subjected to silica gel chromatography and eluted with EtOAc : petroleum ether : CH_2Cl_2 [15 : 1 : 1] to provide **23** as a yellow solid (11.79 g, 90%). ^{1}H NMR (600 MHz, Chloroform-*d*) δ 7.91 (d, 1H, *J* = 13.5 Hz, CH=C), 7.49-7.46 (m, 3H, Ar-H), 7.45 (d, 1H, *J* = 13.5 Hz C=CH), 7.44-7.37 (m, 5H, Ar-H), 7.37-7.34 (m, 2H, Ar-H), 7.13 (dd, 1H, *J* = 8.3, 2.1 Hz, Ar-H), 7.09 (d, 1H, *J* =

2.1 Hz, Ar-H), 6.98 (d, 1H, *J* = 8.3 Hz, Ar-H), 5.25, 5.21 (each s, each 2H, Ar-O-CH_2); ESIMS: calcd for $[M+Na]^+$ *m/z* 384.1; found, 384.2.

*4.4. 2-(3,4-Bis(benzyloxy)phenyl)ethan-1-amine (**24**)*

To a stirring solution of **23** (6.15 g, 17.02 mmol) in anhydrous THF (100 mL) was added a portion of lithium aluminum hydride (4.0 g, 105.52 mmol) at 0 ºC under N_2 atmosphere and the resulting mixture was warmed gradually to 65 ºC. The mixture was stirred overnight at the same temperature until TLC indicated the reaction was complete. After cooling to 0 ºC, the mixture was carefully treated in succession with water (4 mL), 15% NaOH (4 mL) and water again (4 mL). The mixture was filtered through Celite, and the filter cake was washed with tetrahydrofuran. After the filtrate was concentrated under reduced pressure, the residue was diluted with EtOAc, washed with brine, and then dried over Na_2SO_4. The solvent was distilled off, and the resulting oil was purified by flash chromatography [EtOAc : CH_2Cl_2, 1 : 1] to provide **24** as a red oil (3.45 g, 61%). ^{1}H NMR (600 MHz, Chloroform-*d*) δ 7.49-7.45 (m, 4H, Ar-H), 7.38 (dd, 4H, *J* = 8.4, 6.7 Hz, Ar-H), 7.34-7.30 (m, 2H, Ar-H), 6.90 (d, 1H, *J* = 8.1 Hz, Ar-H), 6.81 (d, 1H, *J* = 2.0 Hz, Ar-H), 6.73 (dd, 1H, *J* = 8.1, 2.0 Hz, Ar-H), 5.18, 5.16 (each s, each 2H, Ar-O-CH_2), 2.90 (t, 2H, *J* = 6.8 Hz, N-CH_2), 2.65 (t, 2H, *J* = 6.8 Hz, Ar-CH_2); ESIMS: calcd for $[M+Na]^+$ *m/z* 356.2; found, 356.2.

*4.5. 6,7-Bis(benzyloxy)-1,2,3,4-tetrahydroisoquinoline (**33**)*

To a solution of **24** (2.08 g, 6.24 mmol) in anhydrous MeOH (30 mL) was added 5% paraformaldehyde (237 mg, 7.5 mmol) at room temperature under N_2 atmosphere. After being stirred at 80 ºC for 2 h, trifluoroacetic acid (1 mL, 12.5 mmol) was added to the reaction mixture and kept at the same temperature for 5 h. Then the reaction was neutralized with saturated $NaHCO_3$ solution at 0 °C and then extracted with CH_2Cl_2 three times. The combined organic extracts were washed with water, dried

over Na_2SO_4, concentrated *in vacuo*. A solution of the above crude product in anhydrous MeOH (5 mL) at 0 °C under N_2 atmosphere was treated dropwise with a suspension of sodium borohydride (1.18 g, 31.20 mmol) in anhydrous MeOH (20 mL). The mixture was stirred at r.t. for 5 h and concentrated under reduced pressure. The residue was poured into water and extracted with EtOAc. The combined organic layers were washed with brine, dried over anhydrous Na_2SO_4, filtered, and condensed. The resulting residue was purified via flash chromatography [CH_2Cl_2 : MeOH, 60 : 1] to obtain **33** as a light yellow solid (600 mg, 33%). ^{1}H NMR (600 MHz, Chloroform-*d*) δ 7.48-7.43 (m, 4H, Ar-H), 7.39-7.34 (m, 4H, Ar-H), 7.34-7.29 (m, 2H, Ar-H), 6.69 (s, 1H, Ar-H), 6.61 (s, 1H, Ar-H), 5.13, 5.12 (each s, each 2H, Ar-O-CH_2), 3.92 (s, 2H, Ar-CH_2-N), 3.12 (t, J = 6.0 Hz, 2H, N-CH_2), 2.71 (t, 2H, J = 6.0 Hz, Ar-CH_2); ESIMS: calcd for $[M+Na]^+$ *m/z* 368.2; found, 368.2.

*4.6. 2-(3,4-Bis(benzyloxy)phenyl)ethan-1-ol (**37**)*

Compound **37** was prepared by the procedure used for compound **24** from the known compound methyl 2-(3,4-bis(benzyloxy)phenyl)acetate in 85% yield. ^{1}H NMR (600 MHz, Chloroform-*d*) δ 7.50-7.44 (m, 4H, Ar-H), 7.42-7.35 (m, 4H, Ar-H), 7.35-7.31 (m, 2H, Ar-H), 6.91 (d, 1H, J = 8.1 Hz, Ar-H), 6.85 (d, 1H, J = 2.0 Hz), 6.76 (dd, 1H, J = 8.1, 2.0 Hz, Ar-H), 5.18, 5.16 (each s, each 2H, Ar-O-CH_2), 3.79 (t, 2H, J = 6.5 Hz, O-CH_2), 2.77 (t, 2H, J = 6.5 Hz, Ar-CH_2); ESIMS: calcd for $[M+Na]^+$ *m/z* 357.1; found, 357.1.

*4.7. General procedure for the preparation of compounds (**25-32**), (**34-36**), (**39-40**)*

To a solution of an appropriate acid (0.12 mmol) and related amine or alcohol (0.10 mmol) in an anhydrous CH_2Cl_2 (50 mL) was added EDC·HCl (0.13 mmol) and DMAP (0.01 mmol) at 0 ºC under N_2 atmosphere. Then the mixture was stirred at room temperature for 12 h. The mixture was diluted with CH_2Cl_2, washed with 1 M

HCl, saturated $NaHCO_3$ and brine, dried over Na_2SO_4. After the solvent was distilled off under reduced pressure, the resulting residues were purified by flash chromatography to furnish compounds **25-32**, **34-36**, **39-40**, respectively.

*4.7.1. 2-(Benzyloxy)-N-(3,4-bis(benzyloxy)phenethyl)benzamide (**25**)*

25 was synthesized as a colourless oil in 85% yield. ^{1}H NMR (600 MHz, Chloroform-*d*) δ 8.28 (dd, 1H, *J* = 7.8, 1.9 Hz, Ar-H), 8.01 (t, 1H, *J* = 5.5 Hz, NH), 7.45-7.42 (m, 4H), 7.40-7.34 (m, 8H), 7.33-7.29 (m, 4H), 7.12 (td, 1H, *J* = 7.5, 1.0 Hz, Ar-H), 7.00 (dd, 1H, *J* = 8.4, 1.0 Hz, Ar-H), 6.82 (d, 1H, *J* = 8.1 Hz, Ar-H), 6.79 (d, 1H, *J* = 2.1 Hz, Ar-H), 6.64 (dd, 1H, *J* = 8.1, 2.1 Hz), 5.09, 5.09, 5.08 (each s, each 2H, Ar-O-CH_2), 3.61 (td, 2H, *J* = 7.1, 5.5 Hz, N-CH_2), 2.69 (t, 2H, *J* = 7.1 Hz, Ar-CH_2); HRMS (ESI) calculated for $C_{36}H_{33}NO_4Na$ $(M+Na)^+$ 566.2307, found 566.2311.

*4.7.2. 3-(Benzyloxy)-N-(3,4-bis(benzyloxy)phenethyl)benzamide (**26**)*

26 was synthesized as a white solid in 89% yield. ^{1}H NMR (600 MHz, Chloroform-*d*) δ 7.47-7.42 (m, 5H, Ar-H), 7.42-7.37 (m, 4H, Ar-H), 7.37-7.29 (m, 7H, Ar-H), 7.19 (dt, 1H, *J* = 7.7, 1.2 Hz, Ar-H), 7.13-7.08 (m, 2H), 6.91 (d, 1H, *J* = 8.1 Hz, Ar-H), 6.85 (d, 1H, *J* = 2.0 Hz, Ar-H), 6.76 (dd, 1H, *J* = 8.1, 2.0 Hz, Ar-H), 6.09 (t, 1H, *J* = 5.9 Hz, NH), 5.15, 5.13, 5.10 (each s, each 2H, Ar-O-CH_2), 3.66 (q, 2H, *J* = 6.6 Hz, N-CH_2), 2.84 (t, 2H, *J* = 6.8 Hz, Ar-CH_2) ; HRMS (ESI) calculated for $C_{36}H_{33}NO_4Na$ $(M+Na)^+$ 566.2307, found 566.2312.

*4.7.3. 4-(Benzyloxy)-N-(3,4-bis(benzyloxy)phenethyl)benzamide (**27**)*

27 was synthesized as a white solid in 85% yield. ^{1}H NMR (600 MHz, Chloroform-*d*) δ 7.65 (d, 2H, *J* = 8.8 Hz, Ar-H), 7.47-7.28 (m, 15H, Ar-H), 6.98 (d, 1H, *J* = 8.8 Hz, Ar-H), 6.91 (d, 1H, *J* = 8.1 Hz, Ar-H), 6.85 (d, 1H, *J* = 2.0 Hz, Ar-H), 6.75 (dd, 1H, *J* = 8.1, 2.0 Hz, Ar-H), 6.03 (t, 1H, *J* = 5.8 Hz, NH), 5.16, 5.12, 5.11 (each s, each 2H,

Ar-O-CH_2), 3.65 (q, 2H, *J* = 6.7 Hz, N-CH_2), 2.83 (t, 2H, *J* = 6.8 Hz, Ar-CH_2); HRMS (ESI) calculated for $C_{36}H_{33}NO_4Na$ $(M+Na)^+$ 566.2307, found 566.2313.

*4.7.4. 2,3-Bis(benzyloxy)-N-(3,4-bis(benzyloxy)phenethyl)benzamide (**28**)*

28 was synthesized as a yellow oil in 83% yield. ^{1}H NMR (600 MHz, Chloroform-*d*) δ 8.04 (t, 1H, *J* = 5.7 Hz, NH), 7.80 (dd, 1H, *J* = 7.2, 2.3 Hz, Ar-H), 7.52-7.28 (m, 18H, Ar-H), 7.25-7.21 (m, 2H, Ar-H), 7.20-7.15 (m, 2H, Ar-H), 6.85 (d, 1H, *J* = 8.1 Hz, Ar-H), 6.79 (d, 1H, *J* = 1.9 Hz, Ar-H), 6.67 (dd, 1H, *J* = 8.1, 1.9 Hz, Ar-H), 5.16, 5.12, 5.11, 5.02 (each s, each 2H, Ar-O-CH_2), 3.51 (td, 2H, *J* = 7.2, 5.7 Hz, N-CH_2), 2.64 (t, 2H, *J* = 7.3 Hz, Ar-CH_2); HRMS (ESI) calculated for $C_{43}H_{39}NO_5Na$ $(M+Na)^+$ 672.2726, found 672.2732.

*4.7.5. 3,4-Bis(benzyloxy)-N-(3,4-bis(benzyloxy)phenethyl)benzamide (**29**)*

29 was synthesized as a white solid in 90% yield. ^{1}H NMR (600 MHz, Chloroform-*d*) δ 7.49-7.41 (m, 9H, Ar-H), 7.39-7.28 (m, 12H, Ar-H), 7.10 (dd, 1H, *J* = 8.4, 2.1 Hz, Ar-H), 6.91 (d, 1H, *J* = 8.1 Hz, Ar-H), 6.88 (d, 1H, *J* = 8.4 Hz, Ar-H), 6.84 (d, 1H, *J* = 2.0 Hz, Ar-H), 6.74 (dd, 1H, *J* = 8.1, 2.0 Hz, Ar-H), 5.96 (t, 1H, *J* = 5.9 Hz, NH), 5.20, 5.19, 5.15, 5.12 (each s, each 2H, Ar-O-CH_2), 3.62 (q, 2H, *J* = 6.6 Hz, N-CH_2), 2.82 (t, 2H, *J* = 6.8 Hz, Ar-CH_2); HRMS (ESI) calculated for $C_{43}H_{39}NO_5Na$ $(M+Na)^+$ 672.2726, found 672.2734.

*4.7.6. 3,4,5-Tris(benzyloxy)-N-(3,4-bis(benzyloxy)phenethyl)benzamide (**30**)*

30 was synthesized as a white solid in 84% yield. ^{1}H NMR (600 MHz, Chloroform-*d*) δ 7.47-7.20 (m, 25H, Ar-H), 6.97 (s, 2H, Ar-H), 6.88 (d, 1H, *J* = 7.9 Hz, Ar-H), 6.83 (s, 1H, Ar-H), 6.72 (d, 1H, *J* = 7.9 Hz, Ar-H), 5.94 (d, 1H, *J* = 6.1 Hz, NH), 5.11 (s, 4H, 2 × Ar-O-CH_2), 5.07 (s, 6H, 3 × Ar-O-CH_2), 3.60 (d, 2H, *J* = 6.7 Hz, N-CH_2), 2.80 (t, 2H, *J* = 7.1 Hz, Ar-CH_2); HRMS (ESI) calculated for $C_{50}H_{45}NO_6Na$ $(M+Na)^+$ 778.3145, found 778.3150.

*4.7.7. N-(3,4-Bis(benzyloxy)phenethyl)-2-(3,4-bis(benzyloxy)phenyl)acetamide (**31**)*

31 was synthesized as a white solid in 99% yield. ^{1}H NMR (600 MHz, Chloroform-*d*) δ 7.47-7.28 (m, 20H, Ar-H), 6.86 (d, 1H, *J* = 8.1 Hz, Ar-H), 6.80 (d, 1H, *J* = 8.2 Hz, Ar-H), 6.78 (d, 1H, *J* = 2.1 Hz, Ar-H), 6.72 (d, 1H, *J* = 2.1 Hz, Ar-H), 6.65 (dd, 1H, *J* = 8.2, 2.1 Hz, Ar-H), 6.50 (dd, 1H, *J* = 8.1, 2.1 Hz, Ar-H), 5.32 (t, 1H, *J* = 5.8 Hz, NH), 5.14, 5.12, 5.11, 5.10 (each s, each 2H, Ar-O-CH_2), 3.41 (s, 2H, Ar-CH_2-CO), 3.37 (q, 2H, *J* = 6.8 Hz, NH-CH_2), 2.60 (t, 2H, *J* = 6.9 Hz, Ar-CH_2); HRMS (ESI) calculated for $C_{44}H_{41}NO_5Na$ $(M+Na)^+$ 686.2882, found 686.2892.

*4.7.8. (E)-N-(3,4-Bis(benzyloxy)phenethyl)-3-(3,4-bis(benzyloxy)phenyl)acrylamide (**32**)*

32 was synthesized as a yellow solid in 87% yield. ^{1}H NMR (600 MHz, Chloroform-*d*) δ 7.50 (d, 1H, *J* = 15.5 Hz, Ar-CH=C), 7.48-7.40 (m, 8H, Ar-H), 7.40-7.31 (m, 12H, Ar-H), 7.09 (d, 1H, *J* = 1.8 Hz, Ar-H), 7.04 (dd, 1H, *J* = 8.3, 1.8 Hz, Ar-H), 6.91 (d, *J* = 8.4 Hz, 1H), 6.90 (d, *J* = 8.2 Hz, 1H), 6.83 (d, 1H, *J* = 1.9 Hz, Ar-H), 6.74 (dd, 1H, *J* = 8.2, 1.9 Hz, Ar-H), 6.11 (d, 1H, *J* = 15.5 Hz, CO-CH=C), 5.54 (t, 1H, *J* = 5.8 Hz, NH), 5.20, 5.16, 5.16, 5.15 (each s, each 2H, Ar-O-CH_2), 3.58 (q, 2H, *J* = 6.6 Hz, N-CH_2), 2.78 (t, 2H, *J* = 6.8 Hz, Ar-CH_2); HRMS (ESI) calculated for $C_{45}H_{41}NO_5Na$ $(M+Na)^+$ 698.2882, found 698.2886.

*4.7.9. (6,7-Bis(benzyloxy)-3,4-dihydroisoquinolin-2(1H)-yl)(3,4-bis(benzyloxy)phenyl) methanone (**34**)*

34 was synthesized as a white solid in 82% yield. ^{1}H NMR (600 MHz, Chloroform-*d*) δ 7.48-7.42 (m, 8H, Ar-H), 7.42-.34 (m, 12H, Ar-H), 7.05 (d, 1H, *J* = 1.9 Hz, Ar-H), 7.02 (dd, 1H, *J* = 8.2, 1.9 Hz, Ar-H), 6.96 (d, 1H, *J* = 8.2 Hz, Ar-H), 6.71 (s, 2H, Ar-H), 5.22, 5.20 (each s, each 2H, Ar-O-CH_2), 5.16 (s, 4H, 2 × Ar-O-CH_2), 4.85-4.51

(m, 2H, Ar-CH_2-N), 3.67-3.40 (m, 2H, N-CH_2), 2.68-2.46 (m, 2H, Ar-CH_2); HRMS (ESI) calculated for $C_{44}H_{39}NO_5Na$ $(M+Na)^+$ 684.2726, found 684.2734.

*4.7.10. 1-(6,7-Bis(benzyloxy)-3,4-dihydroisoquinolin-2(1H)-yl)-2-(3,4-bis(benzyloxy)-phenyl)ethan-1-one (**35**)*

35 was synthesized as a white solid in 90% yield. ^{1}H NMR (600 MHz, Chloroform-*d*) δ 7.48-7.42 (m, 12H, Ar-H), 7.40-7.36 (m, 8H, Ar-H), 6.89 (s, 1H, Ar-H), 6.88-6.86 (m, 2H, Ar-H), 6.71 (s, 1H, Ar-H), 6.64 (s, 1H, Ar-H), 5.16 (s, 2H, Ar-O-CH_2), 5.15 (s, 4H, 2 × Ar-O-CH_2), 5.14 (s, 2H, Ar-O-CH_2), 4.58 (s, 2H, Ar-CH_2-N), 3.70 (s, 2H, Ar-CH_2-CO), 3.49 (t, 2H, *J* = 5.8 Hz, N-CH_2), 2.44 (t, 2H, *J* = 5.8 Hz, Ar-CH_2); HRMS (ESI) calculated for $C_{45}H_{41}NO_5Na$ $(M+Na)^+$ 698.2882, found 698.2888.

*4.7.11. (E)-1-(6,7-Bis(benzyloxy)-3,4-dihydroisoquinolin-2(1H)-yl)-3-(3,4-bis-(benzyloxy)phenyl)prop-2-en-1-one (**36**)*

36 was synthesized as a white solid in 94% yield. ^{1}H NMR (600 MHz, Chloroform-*d*) δ 7.60 (d, 1H, *J* = 15.3 Hz, Ar-CH=), 7.51-7.43 (m, 8H, Ar-H), 7.42-7.36 (m, 8H, Ar-H), 7.36-7.30 (m, 4H, Ar-H), 7.14 (s, 1H, Ar-H), 7.11 (d, 1H, *J* = 8.3 Hz, Ar-H), 6.94 (d, 1H, *J* = 8.3 H, Ar-Hz), 6.76 (s, 1H, Ar-H), 6.74 (s, 1H, Ar-H), 6.71 (d, 1H, *J* = 15.3 Hz, CO-CH=), 5.21 (s, 4H, 2 × Ar-O-CH_2), 5.16 (s, 4H, 2 × Ar-O-CH_2), 4.74-4.64 (m, 2H, Ar-CH_2-N), 3.95-3.74 (m, 2H, N-CH_2), 2.86-2.74 (m, 2H, Ar-CH_2); HRMS (ESI) calculated for $C_{46}H_{41}NO_5Na$ $(M+Na)^+$ 710.8258, found 710.8265.

*4.7.12. 3,4-Bis(benzyloxy)phenethyl 2-(3,4-bis(benzyloxy)phenyl)acetate (**39**)*

39 was synthesized as a white solid in 92% yield. ^{1}H NMR (600 MHz, Chloroform-*d*) δ 7.49-7.42 (m, 8H, Ar-H), 7.42-7.32 (m, 8H, Ar-H), 7.35-7.29 (m, 4H, Ar-H), 6.90 (d, 1H, *J* = 2.1 Hz, Ar-H), 6.88 (d, 1H, *J* = 8.2 Hz, Ar-H), 6.86 (d, 1H, *J* = 8.2 Hz, Ar-H), 6.81 (d, 1H, *J* = 2.1 Hz, Ar-H), 6.76 (dd, 1H, *J* = 8.2, 2.1 Hz, Ar-H), 6.67 (dd, 1H, *J* = 8.2, 2.1 Hz, Ar-H), 5.14 (s, 4H, 2 × Ar-O-CH_2), 5.14, 5.13 (each s, each 2H,

Ar-O-CH_2), 4.24 (t, 2H, *J* = 7.0 Hz, N-CH_2), 3.49 (s, 2H, Ar-CH_2-CO), 2.81 (t, 2H, *J* = 7.0 Hz, Ar-CH_2); HRMS (ESI) calculated for $C_{44}H_{40}O_6Na$ $(M+Na)^+$ 687.2723, found 687.2730.

*4.7.13. N-(3,4-Dimethoxyphenethyl)-2-(3,4-dimethoxyphenyl)acetamide (**40**)*

40 was synthesized as a white solid in 95% yield. ^{1}H NMR (600 MHz, Chloroform-*d*) δ 6.79 (dd, *J* = 7.9, 1.6 Hz, 1H), 6.73-6.69 (m, 2H), 6.68 (s, 1H), 6.62 (d, *J* = 1.7 Hz, 1H), 6.53 (dd, *J* = 8.2, 1.7 Hz, 1H), 3.87, 3.84 (each s, each 3H, Ar-O-CH_3), 3.81 (s, 6H, 2 × OCH_3), 3.46 (s, 2H, Ar-CH_2-CO), 3.43 (q, 2H, *J* = 6.5 Hz, N-CH_2), 2.67 (t, 2H, *J* = 7.0 Hz, Ar-CH_2); HRMS (ESI) calculated for $C_{20}H_{25}NO_5Na$ $(M+Na)^+$ 382.1630, found 382.1638.

*4.8. N-(3,4-Dimethoxyphenethyl)-2-(3,4-dimethoxyphenyl)ethanethioamide (**41**)*

To a solution of **40** (200 mg, 0.56 mmol) in 10 mL THF was added Lawesson's reagent (151 mg, 0.61 mmol) at r. t. and the mixture was stirred at reflux for 6 h. After the solvent was evaporated, the residue was purified by flash chromatography [petroleum ether : EtOAc : CH_2Cl_2, 1:1:1] to afford **40** as a yellow oil (208 mg, 99%). ^{1}H NMR (600 MHz, Chloroform-*d*) δ 7.05 (s, 1H, NH), 6.79 (d, 1H, *J* = 8.1 Hz, Ar-H), 6.66 (d, 1H, *J* = 8.2 Hz, Ar-H), 6.63 (dd, 1H, *J* = 8.2, 1.9 Hz, Ar-H), 6.60 (d, 1H, *J* = 1.9 Hz, Ar-H), 6.59 (d, 1H, *J* = 1.9 Hz, Ar-H), 6.41 (dd, 1H, *J* = 8.1, 1.9 Hz, Ar-H), 4.02 (s, 2H, Ar-CH_2-CS), 3.90, 3.87 (each s, each 3H, each OCH_3), 3.85 (t, 2H, *J* = 6.5 Hz, N-CH_2), 3.83, 3.78 (each s, each 3H, each OCH_3), 2.78 (t, *J* = 6.7 Hz, 2H, Ar-CH_2); HRMS (ESI) calculated for $C_{20}H_{25}NSO_4Na$ $(M+Na)^+$ 398.1402, found 398.1410.

*4.9. General procedure for the preparation of compounds (**8-16**), (**18-20**)*

To a solution of compounds **25-32** or **34-36** in MeOH was added a catalytic amount of 10% Pd/C, and the mixture was stirred at room temperature for 12 h under H_2 atmosphere. The reaction mixture was diluted with ether, filtered through Celite. The solvent was distilled off, and the residue was purified by flash chromatography to give compounds **8-16, 18-20** respectively.

*4.9.1. N-(3,4-Dihydroxyphenethyl)-2-hydroxybenzamide (**8**)*

Compound **8** was prepared as a yellow solid in 86% yield. ^{1}H NMR (600 MHz, DMSO-d_6) δ 12.61 (brs, 1H, Ar-OH), 8.85 (t, 1H, J = 5.6 Hz, CO-NH), 8.77 (brs, 1H, Ar-OH), 8.67 (brs, 1H, Ar-OH), 7.82 (dd, 1H, J = 8.0, 1.6 Hz, Ar-H), 7.38 (ddd, 1H, J = 8.5, 7.1, 1.6 Hz, Ar-H), 6.91-6.85 (m, 2H, Ar-H), 6.64 (d, 1H, J = 8.0 Hz, Ar-H), 6.63 (d, 1H, J = 2.1 Hz, Ar-H), 6.48 (dd, 1H, J = 8.0, 2.1 Hz, Ar-H), 3.46-3.41 (m, 2H, N-CH_2), 2.67 (t, 2H, J = 7.5 Hz, Ar-CH_2); ^{13}C NMR (150 MHz, DMSO-d_6) δ 169.23, 160.49, 145.57, 144.06, 134.04, 130.43, 128.11, 119.70, 118.98, 117.81, 116.45, 116.00, 115.73, 41.39, 34.79; HRMS (ESI) calculated for $C_{15}H_{14}NO_4$ $(M-H)^-$ 272.0923, found 272.0945.

*4.9.2. N-(3,4-Dihydroxyphenethyl)-3-hydroxybenzamide (**9**)*

Compound **9** was prepared as a yellow solid in 91% yield. ^{1}H NMR (600 MHz, Chloroform-*d*) δ 9.61 (s, 1H, Ar-OH), 8.75 (s, 1H, Ar-OH), 8.63 (s, 1H, Ar-OH), 8.38 (t, 1H, J = 5.6 Hz, NH), 7.23 (s, 1H, Ar-H), 7.23-7.21 (m, 2H, Ar-H), 6.92-6.86 (m, 1H, Ar-H), 6.64 (d, 1H, J = 8.0 Hz, Ar-H), 6.62 (d, 1H, J = 2.1 Hz, Ar-H), 6.47 (dd, 1H, J = 8.0, 2.1 Hz, Ar-H), 3.41-3.33 (m, 2H, N-CH_2), 2.67-2.59 (m, 2H, Ar-CH_2); ^{13}C NMR (150 MHz, DMSO-d_6) δ 166.58, 157.72, 145.51, 143.95, 136.67, 130.79, 129.65, 119.69, 118.35, 118.04, 116.45, 115.95, 114.65, 41.71, 35.08; HRMS (ESI) calculated for $C_{15}H_{14}NO_4$ $(M-H)^-$ 272.0923, found 272.0945.

*4.9.3. N-(3,4-Dihydroxyphenethyl)-4-hydroxybenzamide (**10**)*

Compound **10** was prepared as a white solid in 95% yield. ^{1}H NMR (600 MHz, DMSO-d_6) δ 9.92 (s, 1H, Ar-OH), 8.75 (s, 1H, Ar-OH), 8.63 (s, 1H, Ar-OH), 8.25 (t, 1H, J = 5.6 Hz, CO-NH), 7.69 (d, 2H, J = 8.6 Hz, Ar-H), 6.78 (d, 2H, J = 8.6 Hz, Ar-H), 6.63 (d, 1H, J = 8.0 Hz, Ar-H), 6.61 (d, 1H, J = 2.1 Hz, Ar-H), 6.46 (dd, 1H, J = 8.0, 2.1 Hz, Ar-H), 3.39-3.31 (m, 2H, N-CH_2), 2.65-2.59 (m, Ar-CH_2); ^{13}C NMR (150 MHz, DMSO-d_6) δ 166.24, 160.40, 145.51, 143.94, 130.87, 129.44(two), 125.88, 119.67, 116.45, 115.95, 115.18 (two), 41.67, 35.28; HRMS (ESI) calculated for $C_{15}H_{14}NO_4$ $(M-H)^-$ 272.0923, found 272.0945.

*4.9.4. N-(3,4-Dihydroxyphenethyl)-2,3-dihydroxybenzamide (**11**)*

Compound **11** was prepared as a purple solid in 86% yield. ^{1}H NMR (600 MHz, DMSO-d_6) δ 12.79 (s, 1H, Ar-OH), 9.12 (s, 1H, Ar-OH), 8.83 (t, 1H, J = 5.7 Hz), 8.76 (s, 1H, Ar-OH), 8.66 (s, 1H, Ar-OH), 8.83 (t, 1H, J = 5.7 Hz, CO-NH), 7.25 (dd, 1H, J = 8.1, 1.4 Hz, Ar-H), 6.90 (dd, 1H, J = 7.8, 1.4 Hz, Ar-H), 6.67 (t, 1H, J = 7.9 Hz, Ar-H), 6.64 (d, 1H, J = 8.0 Hz, Ar-H), 6.62 (d, 1H, J = 2.0 Hz, Ar-H), 6.47 (dd, 1H, J = 8.0, 2.0 Hz, Ar-H), 3.41 (q, 2H, J = 6.6 Hz, N-CH_2), 2.67 (t, 2H, J = 7.6 Hz, Ar-CH_2); ^{13}C NMR (150 MHz, DMSO-d_6) δ 170.08, 150.11, 146.65, 145.56, 144.06, 130.44, 119.70, 119.21, 118.34, 117.58, 116.46, 116.00, 115.48, 41.45, 34.79; HRMS (ESI) calculated for $C_{15}H_{14}NO_5$ $(M-H)^-$ 288.0827, found 288.0875.

*4.9.5. N-(3,4-Dihydroxyphenethyl)-3,4-dihydroxybenzamide (**12**)*

Compound **12** was prepared as a white solid in 93% yield. ^{1}H NMR (600 MHz, DMSO-d_6) δ 8.84 (brs, 4H), 8.16 (t, 1H, J = 5.6 Hz, CO-NH), 7.26 (d, 1H, J = 2.0 Hz, Ar-H), 7.16 (dd, 1H, J = 8.2, 2.0 Hz, Ar-H), 6.74 (d, 1H, J = 8.2 Hz, Ar-H), 6.63 (d, 1H, J = 7.9 Hz, Ar-H), 6.61 (d, 1H, J = 2.0 Hz, Ar-H), 6.45 (dd, 1H, J = 7.0, 2.0 Hz, Ar-H), 3.33 (q, 2H, J = 6.9 Hz, N-CH_2), 2.61 (t, 2H, J = 7.6 Hz, Ar-CH_2); ^{13}C NMR (150 MHz, DMSO-d_6) δ 166.43, 148.64, 145.50, 145.23, 143.92, 130.89, 126.43,

119.66, 119.27, 116.44, 115.95, 115.51, 115.25, 41.66, 35.25; HRMS (ESI) calculated for $C_{15}H_{14}NO_5$ $(M-H)^-$ 288.0827, found 288.0875.

*4.9.6. N-(3,4-Dihydroxyphenethyl)-3,4,5-trihydroxybenzamide (**13**)*

Compound **13** was prepared as a brown solid in 90% yield. ^{1}H NMR (600 MHz, DMSO-d_6) δ 8.75 (s, 5H, Ar-OH), 8.08 (t, 1H, J = 5.6 Hz, CO-NH), 6.80 (s, 2H, Ar-H), 6.63 (d, 1H, J = 8.0 Hz, Ar-H), 6.60 (d, 1H, J = 2.0 Hz, Ar-H), 6.45 (dd, 1H, J = 8.0, 2.0 Hz, Ar-H), 3.33-3.28 (m, 2H, N-CH_2), 2.60 (t, 2H, J = 7.7 Hz, Ar-CH_2); ^{13}C NMR (150 MHz, DMSO-d_6) δ 166.69, 145.84 (two), 145.51, 143.92, 136.57, 130.92, 125.50, 119.68, 116.43, 115.95, 107.12 (two), 41.68, 35.23; HRMS (ESI) calculated for $C_{15}H_{14}NO_6$ $(M-H)^-$ 362.0876, found 362.0887.

*4.9.7. N-(3,4-Dihydroxyphenethyl)-2-(3,4-dihydroxyphenyl)acetamide (**14**)*

Compound **14** was prepared as a white solid in 96% yield. ^{1}H NMR (600 MHz, DMSO-d_6) δ 8.76 (brs, 4H), 7.90 (t, 1H, J = 5.5 Hz, CO-NH), 6.66 (s, 1H, Ar-H), 6.63 (d, 1H, J = 7.9 Hz, Ar-H), 6.62 (d, 1H, J = 7.9 Hz, Ar-H), 6.57 (s, 1H, Ar-H), 6.46 (d, 1H, J = 8.0 Hz), 6.40 (d, 1H, J = 8.0 Hz, Ar-H), 3.18 (s, 2H, Ar-CH_2-CO), 3.16-3.12 (m, 2H, N-CH_2), 2.51-2.49 (m, 2H, Ar-CH_2); ^{13}C NMR (150 MHz, DMSO-d_6) δ 170.97, 145.52, 145.36, 144.23, 143.98, 130.66, 127.60, 120.20, 119.68, 116.93, 116.41, 115.97, 115.79, 42.34, 41.20, 35.18; HRMS (ESI) calculated for $C_{16}H_{16}NO_5$ $(M-H)^-$ 302.1028, found 302.1049.

*4.9.8. N-(3,4-Dihydroxyphenethyl)-3-(3,4-dihydroxyphenyl)propanamide (**15**)*

Compound **15** was prepared as a white solid in 89% yield. ^{1}H NMR (600 MHz, DMSO-d_6) δ 8.67 (s, 4H, Ar-OH), 7.82 (t, 1H, J = 5.7 Hz, CO-NH), 6.62 (d, 1H, J = 8.0 Hz, Ar-H), 6.61 (d, 1H, J = 8.1 Hz, Ar-H), 6.57 (s, 1H, Ar-H), 6.56 (s, 1H, Ar-H), 6.43-6.39 (m, 2H, Ar-H), 3.18-3.12 (m, 2H, N-CH_2), 2.60 (dd, 2H, J = 9.0, 6.7 Hz, Ar-CH_2), 2.50-2.46 (m, 2H, Ar-CH_2), 2.25 (dd, 2H, J = 8.8, 7.0 Hz, CO-CH_2); ^{13}C

NMR (150 MHz, DMSO-d_6) δ 171.79, 145.48, 145.41, 143.93, 143.72, 132.68, 130.75, 119.66, 119.16, 116.40, 116.11, 115.93, 115.87, 41.03, 38.08, 35.20, 31.09; HRMS (ESI) calculated for $C_{17}H_{18}NO_5$ $(M-H)^-$ 316.1185, found 316.1200.

*4.9.9. 3,4-Dihydroxyphenethyl 2-(3,4-dihydroxyphenyl)acetate (**16**)*

Compound **16** was prepared as a yellow solid in 88% yield. ^{1}H NMR (600 MHz, DMSO-d_6) δ 8.78 (s, 4H, Ar-OH), 6.65-6.62 (m, 3H, Ar-H), 6.61 (d, 1H, J = 2.1 Hz, Ar-H), 6.46 (dd, 1H, J = 8.1, 2.1 Hz, Ar-H), 6.44 (dd, 1H, J = 8.0, 2.1 Hz, Ar-H), 4.11 (t, 2H, J = 7.1 Hz, N-CH_2), 3.42 (s, 2H, Ar-CH_2-CO), 2.67 (t, 2H, J = 7.1 Hz, Ar-CH_2); ^{13}C NMR (150 MHz, DMSO-d_6) δ 171.92, 145.54, 145.50, 144.63, 144.22, 128.91, 125.40, 120.47, 119.99, 117.11, 116.65, 115.99, 115.89, 65.48, 40.29, 34.25; HRMS (ESI) calculated for $C_{16}H_{15}O_6$ $(M-H)^-$ 303.0869, found 303.0909.

*4.9.10. (6,7-Dihydroxy-3,4-dihydroisoquinolin-2(1H)-yl)(3,4-dihydroxyphenyl) methanone (**18**)*

Compound **18** was prepared as a white solid in 91% yield. ^{1}H NMR (600 MHz, DMSO-d_6) δ 9.28 (brs, 2H, Ar-OH), 8.84 (brs, 2H, Ar-OH), 6.89-6.70 (m, 3H, Ar-H), 6.52 (s, 2H, Ar-H), 4.46 (s, 2H, Ar-CH_2-N), 3.65-3.53 (m, 2H, N-CH_2), 2.65 (t, 2H, J = 5.7 Hz, Ar-CH_2); ^{13}C NMR (150 MHz, DMSO-d_6) δ 170.12, 147.37, 145.37, 144.41, 144.30, 127.42, 125.01, 124.03, 119.23, 115.81, 115.60, 115.35, 113.46, 51.00, 49.06, 28.41; HRMS (ESI) calculated for $C_{16}H_{14}NO_5$ $(M-H)^-$ 300.0872, found 300.0880.

*4.9.11. 1-(6,7-Dihydroxy-3,4-dihydroisoquinolin-2(1H)-yl)-2-(3,4-dihydroxyphenyl)-ethan-1-one (**19**)*

Compound **19** was prepared as a white solid in 96% yield. ^{1}H NMR (600 MHz, DMSO-d_6) δ 8.86 (brs, 4H, Ar-OH), 6.65-6.61 (m, 2H, Ar-H), 6.51-6.48 (m, 2H, Ar-H), 6.46 (d, 1H, J = 8.1 Hz, Ar-H), 4.40 (s, 2H, Ar-CH_2-N), 3.58 (q, 2H, J = 5.6 Hz, N-CH_2), 3.56 (s, 2H, Ar-CH_2-CO), 2.45 (t, 2H, J = 5.7 Hz, Ar-CH_2); ^{13}C NMR

(150 MHz, DMSO-d_6) δ 170.01, 145.58, 144.25, 126.85, 125.38, 125.00, 124.16, 123.90, 119.93, 116.46, 115.98, 115.61, 113.60, 46.94, 43.87 , 43.71, 28.44; HRMS (ESI) calculated for $C_{17}H_{16}NO_5$ $(M-H)^-$ 314.1028, found 314.1036.

*4.9.12. 1-(6,7-Dihydroxy-3,4-dihydroisoquinolin-2(1H)-yl)-3-(3,4-dihydroxyphenyl) propan-1-one (**20**)*

Compound **20** was prepared as a white solid in 97% yield. ^{1}H NMR (600 MHz, DMSO-d_6) δ 8.74 (brs, 4H, Ar-OH), 6.62-6.60 (m, 2H, Ar-H), 6.51 (s, 1H, Ar-H), 6.50 (s, 1H, Ar-H), 6.47 (s, 1H, Ar-H), 4.39 (s, 1H, Ar-CH_2-N), 3.59 (t, 2H, J = 5.9 Hz, N-CH_2), 3.54 (t, 2H, J = 5.9 Hz, Ar-CH_2), 2.59-2.54 (m, 4H, Ar-C$H_2$$CH_2$); ^{13}C NMR (150 MHz, DMSO-d_6) δ 170.83, 145.42, 144.25, 144.18, 143.74, 132.70, 125.20, 123.96, 119.32, 116.29, 115.86, 115.60, 113.64, 46.40, 43.63, 35.57, 30.64, 28.55; HRMS (ESI) calculated for $C_{18}H_{18}NO_5$ $(M-H)^-$ 328.1185, found 318.1193.

*4.10. N-(3,4-Dihydroxyphenethyl)-2-(3,4-dihydroxyphenyl)ethanethioamide (**17**)*

A solution of **41** (229 mg, 0.61 mmol) in anhydrous dichloromethane (5 mL) was cooled to -78 ºC and 1 M boron tribromide solution in dichloromethane (4.88 mL, 4.88 mmol) was added dropwise under N_2 atmosphere. The reaction was gradually warmed to -40 ºC and stirred for 4 h, and then carefully quenched with cold methanol. After removing the solvents *in vacuum*, the crude residue was purified by flash chromatography [CH_2Cl_2 : MeOH, 8 :1] to get **17** as a yellow oil (171 mg, 88%). ^{1}H NMR (600 MHz, DMSO-d_6) δ 10.07 (t, 1H, J = 5.4 Hz, NH), 8.22 (brs, 1H, Ar-OH), 6.74 (d, 1H, J = 2.0 Hz, Ar-H), 6.68-6.59 (m, 3H, Ar-H), 6.55 (dd, 1H, J = 8.0, 2.0 Hz, Ar-H), 6.44 (dd, 1H, J = 8.0, 2.1 Hz, Ar-H), 3.70 (s, 2H, Ar-CH_2-CS), 3.61 (q, 2H, J = 6.2 Hz, N-CH_2), 2.68 (t, 2H, J = 7.7 Hz, Ar-CH_2); ^{13}C NMR (150 MHz, DMSO-d_6) δ 202.00, 145.59, 145.30, 144.48, 144.14, 130.11, 128.65, 120.09, 119.71, 116.76,

116.37, 116.00, 115.74, 51.41, 47.63, 32.94; HRMS (ESI) calculated for $C_{16}H_{16}NO_4S$ $(M-H)^-$ 318.0800, found 318.0802.

4.11. Cells, viruses and agents

Madin-Darby canine kidney (MDCK) cells were cultured in DMEM (Gibco BRL, USA) supplemented with 10% fetal bovine serum (FBS) (Excell Bio, China), and 1% penicillin/streptomycin (Gibco BRL, USA) at 37 °C with 5% CO_2. The type of influenza A virus applied in this work was A/WSN/33 (H1N1). After infected by the virus, the cells were maintained in FBS-free medium containing 0.6 μg/mL TPCK-Treated Trypsin (SIGMA, USA). Peramivir Trihydrate (Meilun Biological, China) dissolved in DNase/RNase-free ddH_2O to 5 mM as a stock solution was applied as a positive control in the antiviral assay.

4.12. Antiviral assay and microscopy

The inhibitory activity of title compounds against influenza A virus was reviewed by the Thiazolyl Blue Tetrazolium Bromide (MTT) (SIGMA, USA) assay [35]. MDCK cells were seeded into a 96-well tissue culture plate overnight, and then infected with a 100 tissue culture infective doses ($TCID_{50}$) (MOI=3.5×10^{-3}) for 1 h. The test compounds were added to the infected cells with increasing amounts and then cultivated about 48 h. MTT solution (5 mg/ mL) in PBS was added to each well. Prior to detection, DMSO was added to dissolve the formazan crystals. And the absorbance was recorded by a microplate reader (GENios Pro, TECAN, Bedford, MA, USA) at 570 nm. In addition, the cytopathic effect (CPE) that induced by the virus was observed by microscopy.

4.13. Cytotoxicity assay

MDCK cells were grown in a 96-well tissue culture plate overnight. Diluted test compounds with increasing amounts or blank control solutions (0.1% DMSO) were

supplemented in cells. After 48 h, the cytotoxicity of the test compounds was submitted to the MTT assay as previously described [36]. The concentration of the test compounds that resulted in the death of 50% cells was recognized as the 50% cytotoxic concentration (CC_{50}).

4.14. Endonuclease activity assay

The PA_N endonuclease (MyBiosource MBS7111040, San Diego, USA) assay was performed as described previously [37, 38]. The influenza A PA_N domain has been shown to cleave ssRNA as well as ssDNA. A TaqMan-like oligonucleotide was used containing a 6-carboxy-fluorescein (FAM) fluorophore at the 5'-end followed by 19 nucleotides and a minor groove binding non-fluorescent quencher (MGBNFQ, Applied Biosystems) at the 3'-end. When excited by light at a wavelength of 492 nm, MGBNFQ quenches the fluorescence of FAM via fluorescence resonance energy transfer. If the endonuclease cleaves the oligonucleotide, the quencher is no longer coupled to the fluorophore, and therefore, FAM fluoresces. The assay can be used to evaluate the inhibitory characteristics of compounds that are found to bind PA_N. The assay uses the probe 6FAM-TGGCAATATCAGCTCCACA-MGBNFQ. EGCG and BXA were included as a reference compound, respectively.

4.15. Surface Plasmon Resonance (SPR) Measurement

In order to study the interaction between candidate compounds and H1N1 virus PA_N endonuclease (MyBiosource MBS7111040, San Diego, USA), we performed an affinity measurement by means of Surface Plasmon Resonance (SPR) technology. The SPR validation experiment was perform with the Screen LB 991 Label-free Microarray System (BERTHOLD TECHNOLOGIES, Germany). The chemical modified label-free photo-cross-linker sensor chips were provided by Betterways Inc.

(China). For array spotting, BioDot™ AD-1520 Array Printer (BIODOT Inc., USA) was employed to printed samples and control EGCG as well as BXA (Figure S2) on the surface. Each candidate compound was printed with a volume of 1.875 nL/dot using BioDot 1520 array printer with the formation of 5 nonadjacent repetitions of each sample in the same chip. During the SPR test, the surface was first primed three times with HBS-EP running buffer (containing 10 mM HEPES, pH 7.0, 150 mM NaCl, 3 mM EDTA and 0.005% (v/v) of P20 surfactant) at rate of 2 μL/s for 40 s and one time with running buffer (1 × PBS with 5% DMSO) at rate of 2 μL/s for 40 s. The PA_N endonuclease (MyBiosource, San Diego, USA) was diluted separately with running buffer at the concentration of 10 nM, 20 nM, 40 nM, 80 nM and 160 nM and injected for 600 s at a flow rate of 0.5 μL/s using in each associating stage, followed by running buffer for 360 s at a flow rate of 0.5 μL/s in each dissociating stage. The raw sensor grams and measurements of the binding process of ligands and proteins were recorded in real time. The response unit (RU) of surface resonance was compared to determine the different binding affinity between each sample. The equilibrium dissociation constant (K_D) was performed using data analysis software of the Screen LB 991 unlabeled microarray system according to a single-site binding model (1:1 Langmuir binding) with mass transfer limitations for determination of the binding kinetics.

4.16. Molecular docking

All calculations were performed using SYBYL 7.3 [39]. The protein structure of H1N1 virus PA_N endonuclease bound with BXA (PDB ID: 6FS6) [40] was applied for

docking study. The 3D structures of target compounds were constructed using the Discovery Studio small molecule window. And the hydrogen and Gasteiger-Hückel charges were added to target compounds. Then the energy was minimized by MMFF94 force field in two step methods: steepest descent with RMS gradient convergent to 0.1, and the final step was conjugate gradient with RMS gradient convergent to 0.0001. Prior to the docking procedure, all superfluous bound water molecules were removed from the protein crystal structure. The docking program surflex-dock was used to perform the automated molecular simulation in which the top hits were set as 10, and the random conformations were set as 10. The top compounds were ranked by the corresponding values of Total_Score and CSCORE.

References

[1] C. Cianci, S.W. Gerritz, C. Deminie, M. Krystal, Influenza nucleoprotein: promising target for antiviral chemotherapy, Antivir. Chem. Chemother. 23 (2012) 77-91.

[2] R.A. Bright, M.J. Medina, X. Xu, G. Peresz-Oronoz, T.R. Wallis, X.M. Davis, L. Provinelli, N.J. Cox, A.I. Klimov, Incidence of admantane resistance among influenza A (H3N2) viruses isolated worldwide from 1994 to 2005: a cause for concern, Lancet 366 (2005) 1175-1181.

[3] A. Moscona, Oseltamivir eesistance-disabling our influenza defenses, N. Engl. J. Med. 353 (2005) 2633-2636.

[4] J.D. Bloom, L.I. Gong, D. Baltimore, Permissive secondary mutations enable the evolution of influenza oseltamivir resistance, Science 328 (2010) 1272-1275.

[5] M.J. Memoli, A.S. Davis, K. Proudfoot, D.S. Chertow, R.J. Hrabal, T. Bristol, J.K. Taubenberger, Multidrug-resistant 2009 pandemic influenza A(H1N1) viruses maintain fitness and transmissibility in ferrets, J. Infect. Dis. 203 (2011) 348-357.

[6] P. Palese, J.L. Schulman, Mapping of the influenza virus genome: identification of the hemagglutinin and the neuraminidase genes, Proc Natl Acad Sci U. S. A. 73 (1976) 2142-2146.

[7] P. Palese, M.B. Ritchey, J.L. Schulman, Mapping of the influenza virus genome. II. identification of the P1, P2, and P3 genes, Virology 76 (1977) 114-121.

[8] T.S. Huang, P. Palese, M. Krystal, Determination of influenza virus proteins required for genome replication, J. Virol. 64 (1990) 5669-5673.

[9] E. Fodor, The RNA polymerase of influenza a virus: mechanisms of viral transcription and replication. Acta. Virol. 57 (2013) 113-122.

[10] K. Das, J.M. Aramini, L.C. Ma, R.M. Krug, E. Arnold, Structures of influenza A proteins and insights into antiviral drug targets, Nat. Struct. Mol. Biol. 17 (2010) 530-538.

[11] A. Dias, D. Bouvier, T. Crépin, A.A. McCarthy, D.J. Hart, F. Baudin, S. Cusack, R.W. Ruigrok, The cap-snatching endonuclease of influenza virus polymerase resides in the PA subunit, Nature 458 (2009) 914-918.

[12] R.M. DuBois, P.J. Slavish, B.M. Baughman, M.K. Yun, J. Bao, R.J. Webby, T.R. Webb, S.W. White, Structural and biochemical basis for development of influenza virus inhibitors targeting the PA endonuclease, PLoS. Pathog. 8 (2012) e1002830.

[13] E. Kowalinski, C. Zubieta, A. Wolkerstorfer, O.H. Szolar, R.W. Ruigrok, S. Cusack, Structural analysis of specific metal chelating inhibitor binding to the endonuclease domain of influenza pH1N1 (2009) polymerase, PLoS Pathog. 8 (2012) e1002831.

[14] J. Tomassini, H. Selnick, M.E. Davies, M.E. Armstrong, J. Bladwin, M. Bourgeois, J. Hastings, D. Hazuda, J. Lewis, W. McClements, G. Ponticello, E. Radzilowski, G. Smith, A. Tebben, A. Wolfe, Inhibition of cap (m7GpppXm)-dependent endonuclease of influenza virus by 4-substituted 2,4-dioxobutanoic acid compounds, Antimicrob. Agents. Chemother. 38 (1994) 2827-2837.

[15] J.C. Hastings, H. Selnick, B. Wolanski, J.E. Tomassini, Anti-influenza virus activities of 4-substituted 2,4-dioxobutanoic acid inhibitors, Antimicrob. Agents. Chemother. 40 (1996) 1304-1307.

[16] M. Carcelli, D. Rogolino, A. Bacchi, G. Rispoli, E. Fisicaro, C. Compari, M. Sechi, A. Stevaert, L. Naesens, Metal-chelating 2-hydroxyphenyl amide pharmacophore for inhibition of influenza virus endonuclease, Mol. Pharm. 11 (2014) 304-316.

[17] J.E. Tomassini, M.E. Davies, J.C. Hastings, R. Lingham, M. Mojena, S.L. Raghoobar, S.B. Singh, J.S. Tkacz, M.A. Goetz, A novel antiviral agent which inhibits the endonuclease of

influenza viruses, Antimicrob. Agents. Chemother. 40 (1996) 1189-1193.

[18] E. Chen, R.V. Swift, N. Alderson, V.A. Feher, G.S., Feng, R.E. Amaro, Computation-guided discovery of influenza endonuclease inhibitors, ACS Med. Chem. Lett. 5 (2014) 61-64.

[19] H.Y. Sagong, A. Parhi, J.D. Bauman, D. Patel, R.S. Vijayan, K. Das, E. Arnold, E.J. LaVoie, 3-Hydroxyquinolin-2(1H)-ones as inhibitors of influenza A endonuclease, ACS Med. Chem. Lett. 4 (2013) 547-550

[20] J.D. Bauman, D. Patel, S.F. Baker, R.S. Vijayan, A. Xiang, A.K. Parhi, L. Martínez-Sobrido, E.J. LaVoie, K. Das, E. Arnold, Crystallographic fragment screening and structure-based optimization yields a new class of influenza endonuclease inhibitors, ACS Chem. Biol. 8 (2013) 2501-2508.

[21] H.Y. Sagong, J.D. Bauman, D. Patel, K. Das, E. Arnold, E.J. LaVoie, Phenyl substituted 4-hydroxypyridazin-3(2H)-ones and 5-hydroxypyrimidin-4(3H)-ones: inhibitors of influenza A endonuclease, J. Med. Chem. 57 (2014) 8086-8098.

[22] C.V. Credille, Y. Chen, S.M. Cohen, Fragment-based identification of influenza endonuclease inhibitors, J. Med. Chem. 59 (2016) 6444-6454.

[23] M. Miyagawa, T. Akiyama, Y. Taoda, K. Takaya, C. Takahashi-Kageyama, K. Tomita, K. Yasuo, K. Hattori, S. Shano, R. Yoshida, T. Shishido, T. Yoshinaga, A. Sato, M. Kawai, Synthesis and SAR study of carbamoyl pyridone bicycle derivatives as potent inhibitors of influenza cap-dependent endonuclease, J. Med. Chem. 62 (2019) 8101-8114.

[24] T. Noshi, M. Kitano, K. Taniguchi, A. Yamamoto, S. Omoto, K. Baba, T. Hashimoto, K. Ishida, Y. Kushima, K. Hattori, M. Kawai, R. Yoshida, M. Kobayashi, T. Yoshinaga, A. Sato M. Okamatsu, Y. Sakoda, H. Kida, T. Shishido, A. Naito, In vitro characterization of baloxavir acid, a first-in-class cap-dependent endonuclease inhibitor of the influenza virus polymerase PA subunit, Antiviral. Res. 160 (2018) 109-117.

[25] R. O'Hanlon, M.L. Shaw, Baloxavir marboxil: the new influenza drug on the market, Curr. Opin. Virol. 35 (2019) 14-18.

[26] M. Imai, M. Yamashita, Y. Sakai-Tagawa, K. Iwatsuki-Horimoto, M. Kiso, J. Murakami, A. Yasuhara, K. Takada, M. Ito, N. Nakajima, K. Takahashi, T.J.S. Lopes, J. Dutta, Z. Khan, D. Kriti, H. van Bakel, A. Tokita, H. Hagiwara, N. Izumida, H. Kuroki, T. Nishino, N. Wada, M. Koga, E. Adachi, D. Jubishi, H. Hasegawa, Y. Kawaoka . Influenza A variants with reduced

susceptibility to baloxavir isolated from Japanese patients are fit and transmit through respiratory droplets, Nat. Microbiol. 5 (2020) 27-33.

[27] T. Kuzuhara, Y. Iwai, H. Takahashi, D. Hatakeyama, N. Echigo, Green tea catechins inhibit the endonuclease activity of influenza A virus RNA polymerase, PLoS. Curr. 1 (2009) RRN1052.

[28] Y. Iwai, K. Murakami, Y. Gomi, T. Hashimoto, Y. Asakawa, Y. Okuno, T. Ishikawa, D. Hatakeyama, N. Echigo, T. Kuzuhara, Anti-influenza activity of marchantins, macrocyclic bisbibenzyls contained in liverworts, PLoS One 6 (2011) e19825.

[29] S. Fudo, N. Yamamoto, M. Nukaga, T. Odagiri, M. Tashiro, S. Neya, T. Hoshino, Structural and computational study on inhibitory compounds for endonuclease activity of influenza virus polymerase, Bioorg. Med. Chem. 23 (2015) 5466-5475.

[30] Y. Iwai, H. Takahashi, D. Hatakeyama, K. Motoshima, M. Ishikawa, K. Sugita, Y. Hashimoto, Y. Harada, S. Itamura, T. Odagiri, M. Tashiro, Y. Sei, K. Yamaguchi, T. Kuzuhara, Anti-influenza activity of phenethylphenylphthalimide analogs derived from thalidomide, Bioorg. Med. Chem. 18 (2010) 5379-5390.

[31] N. Pala, A. Stevaert, R. Dallocchio, A. Dessì, D. Rogolino, M. Carcelli, V. Sanna, M. Sechi, L. Naesens, Virtual screening and biological validation of novel influenza virus PA endonuclease inhibitors, ACS Med. Chem. Lett. 6 (2015) 866-871.

[32] S. Ferro, R. Gitto, M.R. Buemi, S. Karamanou, A. Stevaert, L. Naesens, L. De Luca, Identification of influenza PA-Nter endonuclease inhibitors using pharmacophore-and docking-based virtual screening, Bioorg. Med. Chem. 26 (2018) 4544-4550.

[33] W.H. Zhan, L. Xu, X.W. Dong, J. Dong, X. Yi, X.D. Ma, N. Qiu, J. Li, B. Yang, Y.B. Zhou, Y.Z. Hu, Design, synthesis and biological evaluation of pyrazol-furan carboxamide analogues as novel akt kinase inhibitors, Eur. J. Med. Chem. 117 (2016) 47-58.

[34] Y.X. Liao, Y.M. Guo, S.M. Li, L. Wang, Y.M. Tang, T.M. Li, W.H. Chen, G.H. Zhong, G.P. Song, Structure-based design and structure-activity relationships of 1,2,3,4-tetrahydroisoquinoline derivatives as potential PDE4 inhibitors, Bioorg. Med. Chem. Lett. 28 (2018) 1188-1193.

[35] T. Liu, M.M. Liu, F.M. Chen, F.Z. Chen, Y.X. Tian, Q. Huang, S.W. Liu, J. Yang, Small-molecule compound has anti-influenza A virus activity by acting as a “PB2 Inhibitor”,

Mol. Pharm. 15 (2018) 4110-4120

[36] C.F. Hsieh, C.W. Lo, C.H. Liu, S. Lin, H.R. Yen, T.Y. Lin, J.T. Horng, Mechanism by which ma-xing-shi-gan-tang inhibits the entry of influenza virus, J. Ethnopharmacol. 143 (2012) 57-67.

[37] H.Y. Sagong, A. Parhi, J.D. Bauman, D. Patel, R.S. Vijayan, K. Das, E. Arnold, E.J. LaVoie, 3-Hydroxylquinolin-2(1H)-ones as inhibitors of influenza A endonuclease, ACS Med. Chem. Lett. 4 (2013) 547-550.

[38] E. Noble, A. Cox, J. Deval, B. Kim, Endonuclease substrate selectivity characterized with full-length PA of influenza A virus polymerase. Virology. 433 (2012) 27-34.

[39] Y.X. Liao, L.Z. Chen, S.M. Li, Z.N. Cui, Z.W. Lei, H. Li, S.W. Liu, G.P. Song, Structure-aided optimization of 3-O-β-chacotriosyl ursolic acid as novel H5N1 entry inhibitors with high selective index, Bioorg. Med. Chem. 27 (2019) 4048-4058.

[40] S. Omoto, V. Speranzini, T. Hashimoto, T. Noshi, H. Yamaguchi, M. Kawai, K. Kawaguchi, T. Uehara, T. Shishido, A. Naito, S. Cusack, Characterization of influenza virus variants induced by treatment with the endonuclease inhibitor baloxavir marboxil, Sci. Rep. 8 (2018) 9633-9647.

Acknowledgements

This project was supported by the National Nature Science Foundation of China (Grant No. 31572565, 21202047), the Natural Science Foundation of Guangdong Province, China (2018A030313414) and Science &Technology Project of Guangzhou, China (201804010457).

Table 1. In Vitro Anti-Influenza A Virus Activities of the polyphenols derivatives (**8-17**)

compd	n	X	Y	R1	R2	R3	R4	EC_{50}[a](μM)	CC_{50}[b](μM)	SI
8	0	O	NH	OH	H	H	H	>30	N.D.	N.D.
9	0	O	NH	H	OH	H	H	13.08±5.17	>200	>15.3
10	0	O	NH	H	H	OH	H	12.67±4.46	>200	>25.2
11	0	O	NH	OH	OH	H	H	>30	N.D.	N.D.
12	0	O	NH	H	OH	OH	H	10.23±4.77	153.60±19.10	15.0
13	0	O	NH	H	OH	OH	OH	>30	N.D.	N.D.
14	1	O	NH	H	OH	OH	H	2.46±0.82	>200	>81.3
15	2	O	NH	H	OH	OH	H	4.94±1.84	>200	>64.8
16	1	S	NH	H	OH	OH	H	>30	N.D.	N.D.
17	1	O	O	H	OH	OH	H	7.01±3.59	>200	>45.7
EGCG								28.93±1.38	>200	>6.9
Peramivir								5.26±2.19	>200	>38.0

[a]The samples were examined in MDCK cells in triplicate. MDCK cells were incubated with test compounds and influenza A virus (A/WSN/33), and the concentration of test compound resulting in 50% cell protection was reported as the EC_{50}. [b]50% cellular cytotoxicity concentration. N.D., not determined.

Table 2. In Vitro Anti-Influenza A Virus Activities of the polyphenols derivatives (**18-20**)

compd	n	EC_{50}[a](μM)	CC_{50}[b](μM)	SI
18	0	3.10±1.10	133.15±30.65	43.0
19	1	2.58±0.98	150.85±9.95	58.5
20	2	18.61±12.0	197.20±15.90	10.6
EGCG		28.93±1.38	>200	>6.9
Peramivir		5.26±2.19	>200	>38.0

[a]The samples were examined in MDCK cells in triplicate. MDCK cells were incubated with test compounds and influenza A virus (A/WSN/33), and the concentration of test compound resulting in 50% cell protection was reported as the EC_{50}. [b]50% cellular cytotoxicity concentration.

Table 3. Inhibitory activity of the potential compounds and reference compound EGCG and BXA against influenza PA_N endonuclease.

compd	EC_{50}[a] (nM)
14	312.36±12.05
15	842.14±19.28
17	1294.56±78.43
18	576.85±42.59
19	489.39±33.35
EGCG	6454.75±506.12
BXA	1.34±0.11

[a]Data shown are the mean ± SD of eleven independent experiments.

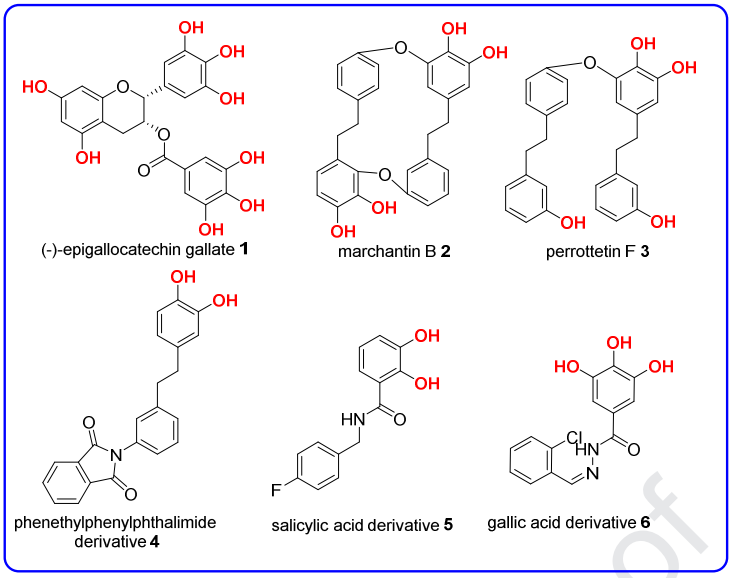

Figure 1. Early polyphenols endonuclease inihibitors.

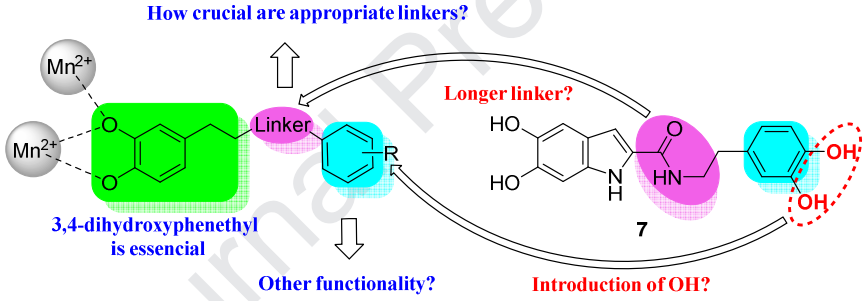

Figure 2. SARs of polyphenols derivatives starting point and chemical structure of **7**

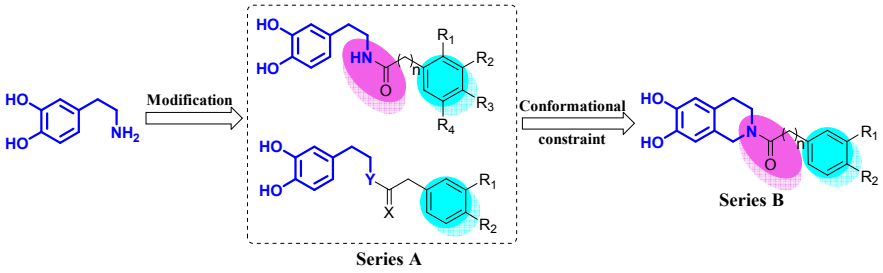

Figure 3. Design strategy of novel influenza virus endonuclease inhibitor.

Scheme 1. Synthesis of polyphenols derivatives **8-15**, **18-20**[a]

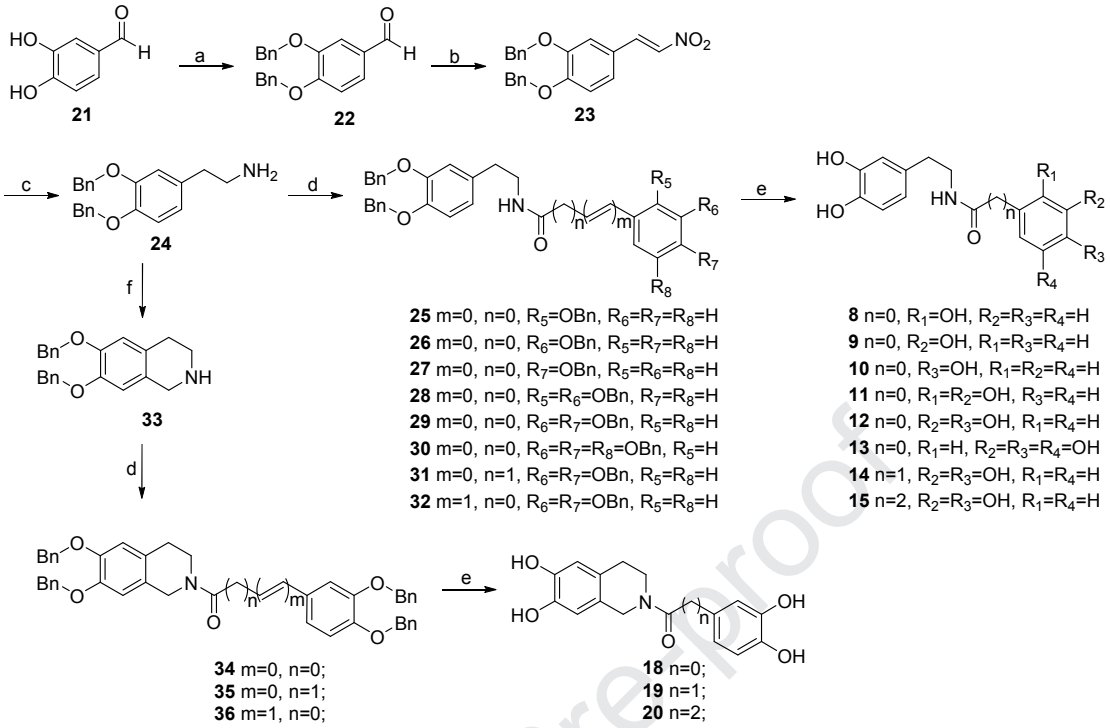

[a]Reagents and conditions: Reagents and conditions: (a) BnBr, K_2CO_3, DMF, 65 ^oC, 10 h; (b) CH_3NO_2, AcOH, NH_4OAc, 90 ^oC, 5 h; (c) LAH, dry THF, 0 ^oC, 30 min, 65 ^oC, overnight; (d) carboxylic acid, DMAP, EDC·HCl, 0 ^oC to rt, overnight; (e) H_2, 10% Pd/C, MeOH, overnight; (f) i. Paraformaldehyde, MeOH, 80 ^oC, 2 h; ii. TFA, 5h; iii. $NaBH_4$, MeOH, 0 ^oC to rt, overnight.

Scheme 2. Synthesis of polyphenols derivative **16-17**[a]

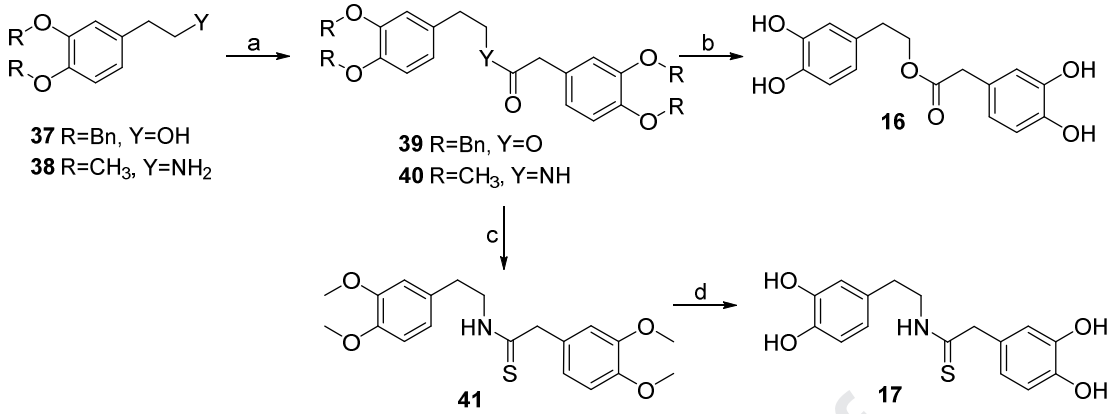

[a]Reagents and conditions: (a) carboxylic acid, DMAP, EDC·HCl, 0 °C to rt, overnight; (b) H_2, 10% Pd/C, MeOH, rt, 12 h; (b) Lawesson's reagent, dry THF, 66 °C, 6 h; (d) BBr_3, dry CH_2Cl_2, -78 °C to -40 °C, 5-6 h.

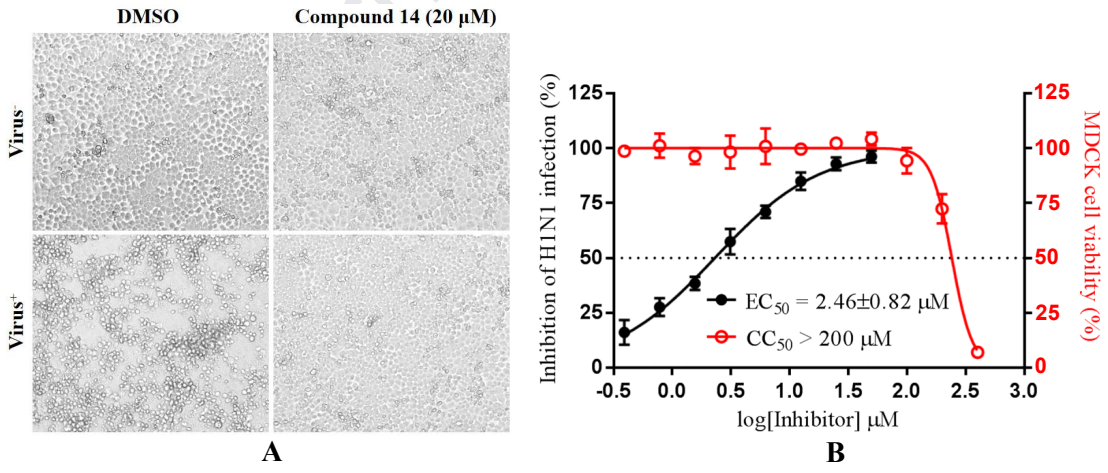

Figure 4. (A) Validation of the protection of MDCK cells from influenza A/WSN/33 virus by compound **14**. (B) Dose-response curve for potential compound **14** in the antiviral and cytotoxicity assay.

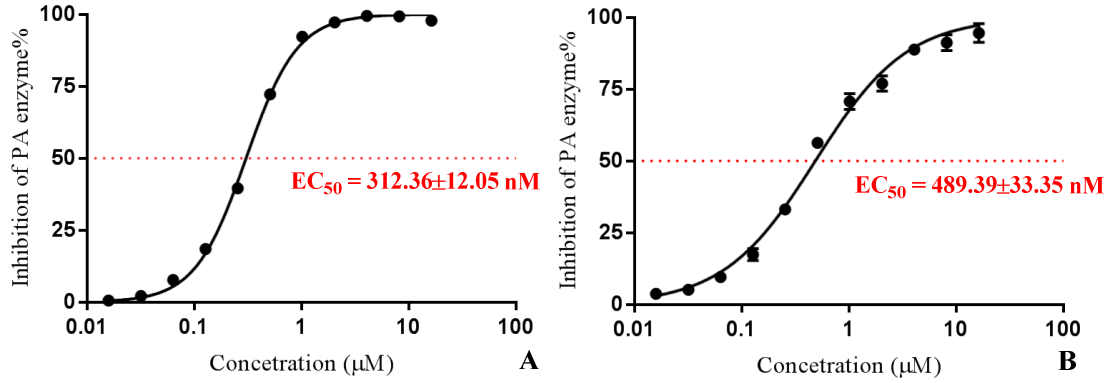

Figure 5. Dose-response curve for potential compound **14** (A) and **19** (B) in the enzymatic assay with recombinant PA-Nter endonuclease. The percentage inhibition of PA_N endonuclease activity was plotted against the compound concentration on a semilogarithmic plot. Data shown are the mean ± SD of eleven independent experiments.

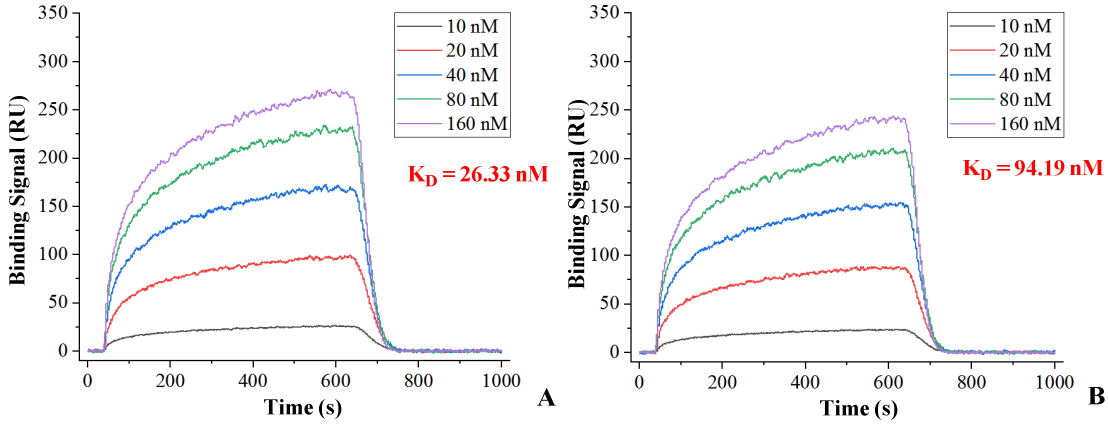

Figure 6. Characterization of the affinity between potential compound **14** (A) and **19** (B) and PA_N endonuclease, based on the SPR assay. Their K_D values are labeled in the corresponding curves.

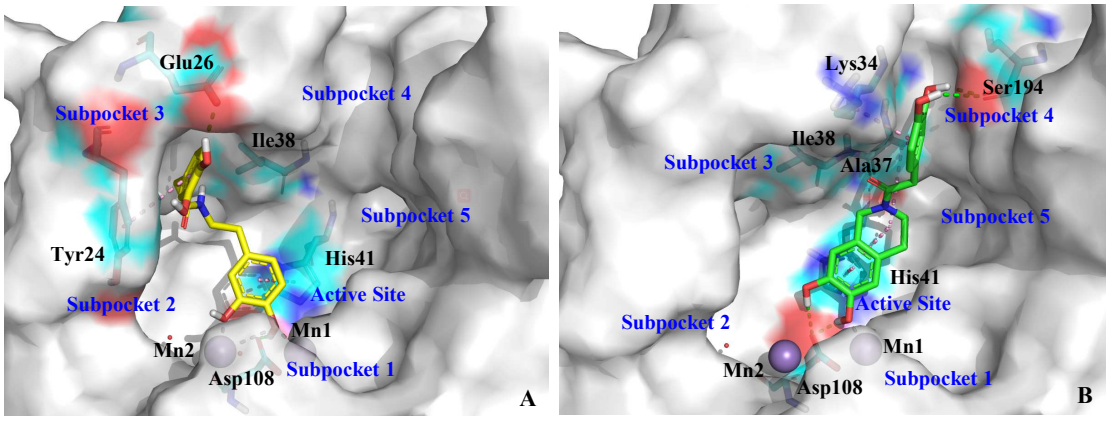

Figure 7. Structural representative of **14** and **19** binding within PA protein (Protein Data Bank: 6FS6) according to surflex-dock calculation. Residues are represented by cyan stick. The coloring is described as follow: C atoms of **14** and **19** are colored in yellow and green, respectively; Red, oxygen atom of **14** and **19** and water molecule in catalytic pocket; Mazarine, manganese ion; Blue, nitrogen atom. The H-bonds, pi-pi stacked and metal-coordinating bonds are shown in green dashed lines, pink dashed lines and gray dashed lines, respectively.

Research Highlights

The new class of dopamine-based PA_N endonuclease inhibitors were rationally designed;

Compounds were found to possess strong anti-IAV activity and low cytotoxicity;

Mechanistic studies revealed that compound **14** could tightly bind with PA_N protein;

Biological data are well consistent with docking results suggesting mechanism of action.

Declaration of interests

☒ The authors declare that they have no known competing financial interests or personal relationships that could have appeared to influence the work reported in this paper.

☐The authors declare the following financial interests/personal relationships which may be considered as potential competing interests:

We declare that we have no known competing financial interests or personal relationships that could have appeared to influence the work reported in this paper.
All the authors agree to submit our manuscript to *European journal of medicinal chemistry.*